

This article is published as part of the *Dalton Transactions* themed issue entitled:

# Dalton Transactions 40th Anniversary

Guest Editor Professor Chris Orvig, Editorial Board Chair  
University of British Columbia, Canada

Published in issue 40, 2011 of *Dalton Transactions*

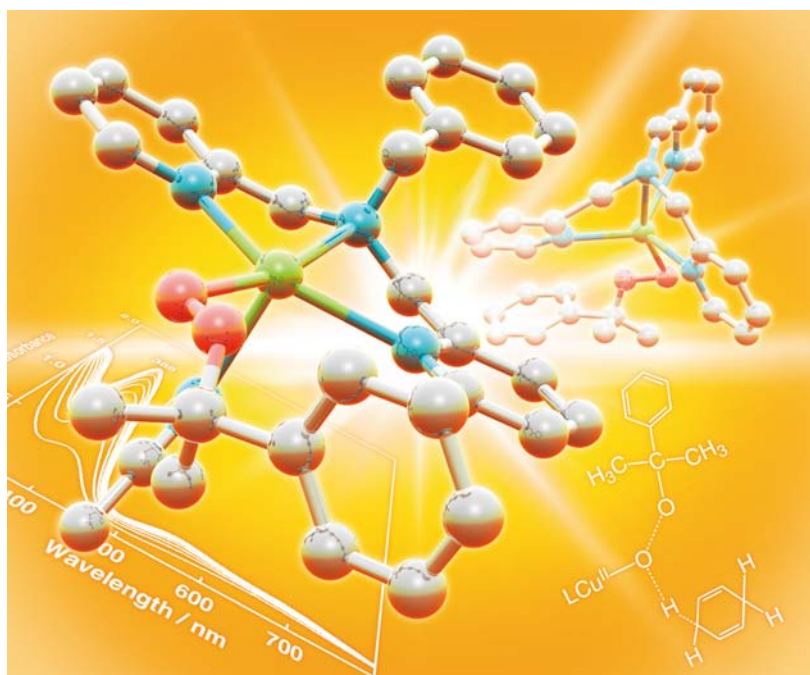


Image reproduced with permission of Shinobu Itoh

Welcome to issue 40 of the 40th volume of *Dalton Transactions*-40/40! Articles in the issue include:

## PERSPECTIVE:

[Synthesis and coordination chemistry of macrocyclic ligands featuring NHC donor groups](#)

Peter G. Edwards and F. Ekkehardt Hahn  
*Dalton Trans.*, 2011, 10.1039/C1DT10864F

## FRONTIER:

[The future of metal–organic frameworks](#)

Neil R. Champness  
*Dalton Trans.*, 2011, DOI: 10.1039/C1DT11184A

## ARTICLES:

[Redox reactivity of photogenerated osmium\(II\) complexes](#)

Jillian L. Dempsey, Jay R. Winkler and Harry B. Gray  
*Dalton Trans.*, 2011, DOI: 10.1039/C1DT11138H

[Molecular squares, cubes and chains from self-assembly of bis-bidentate bridging ligands with transition metal dications](#)

Andrew Stephenson and Michael D. Ward  
*Dalton Trans.*, 2011, DOI: 10.1039/C1DT10263J

Visit the *Dalton Transactions* website for more cutting-edge inorganic and organometallic research

[www.rsc.org/dalton](http://www.rsc.org/dalton)

**Bis(2-pyridylimino)isoindolato iron(II) and cobalt(II) complexes: Structural chemistry and paramagnetic NMR spectroscopy†**

Matthias Kruck, Désirée C. Sauer, Markus Enders, Hubert Wadepohl and Lutz H. Gade\*

Received 11th April 2011, Accepted 13th May 2011

DOI: 10.1039/c1dt10617a

Condensation of phthalodinitrile and 2-amino-5,6,7,8-tetrahydroquinoline gave the bis(2-pyridylimino)isoindole protioligand **1** (thqbpH) in high yield. Deprotonation of thqbpH (**1**) using LDA in THF at  $-78\text{ }^{\circ}\text{C}$  yields the corresponding lithium complex [Li(THF)(thqbp)] (**2**) in which the lithium atom enforces almost planar arrangement of the tridentate ligand, with an additional molecule of THF coordinated to Li. Reaction of cobalt(II) chloride or iron(II) chloride with one equivalent of the lithium complex **2** in THF led to formation of the metal complexes [CoCl(THF)(thqbp)] (**3a**) and [FeCl(THF)(thqbp)] (**3b**). The paramagnetic susceptibility of **3a,b** in solution was measured by the Evans method (**3a**:  $\mu_{\text{eff}} = 4.17\ \mu_{\text{B}}$ ; **3b**:  $\mu_{\text{eff}} = 5.57\ \mu_{\text{B}}$ ). Stirring a solution of **1** and cobalt(II) acetate tetrahydrate in methanol yielded the cobalt(II) complex **4** which was also accessible by treatment of **3a** with one equivalent of silver or thallium acetate in DMSO. Whereas **3a,b** were found to be mononuclear in the solid state, the acetate complex **4** was found to be dinuclear, the two metal centres being linked by an almost symmetrically bridging acetate. For all transition metal complexes paramagnetic  $^1\text{H}$  as well as  $^{13}\text{C}$  NMR spectra were recorded at variable temperatures. The complete assignment of the paramagnetic NMR spectra was achieved by computation of the spin densities within the complexes using DFT. The proton NMR spectra of **3a** and **3b** displayed dynamic behaviour. This was attributed to the exchange of coordinating solvent molecules by an associative mechanism which was analysed using lineshape analysis ( $\Delta S^{\ddagger} = -154 \pm 25\ \text{J mol}^{-1}\ \text{K}^{-1}$  for **3a** and  $\Delta S^{\ddagger} = -168 \pm 15\ \text{J mol}^{-1}\ \text{K}^{-1}$  for **3b**).

**Introduction**

During the past decade there has been a renaissance of molecular catalysis using late 3d transition metals instead of the precious platinum metals, which has given rise to a range of novel classes of catalysts.<sup>1</sup> This has entailed the development of appropriate ancillary ligand systems which on the one hand stabilise the molecular catalyst and on the other hand create a well defined active space around the metal centre. The key elements of ligand design for this purpose have been the combination of ligand architecture (denticity and construction of the ligand backbone) and the choice of ligating atoms. For the 3d transition metals nitrogen donor ligands have proved to meet the requirements for the development of active and stable catalysts.<sup>2</sup>

Monoanionic meridionally coordinating tridentate ligands, frequently referred to as “pincers”, have been extensively studied in development of novel molecular catalysts.<sup>3</sup> Bis(2-pyridylimino)isoindoles (bpi) are highly modular, readily accessible

ligands of this type. They were first reported in the 1950s<sup>4</sup> and their coordination chemistry has been investigated since the 1970s.<sup>5</sup> Several examples of applications of these ligands in catalysis have been reported, including the cobalt-catalysed aerobic oxidation of hydrocarbons,<sup>6</sup> the palladium-catalysed hydrogenation of C=C bonds<sup>7</sup> as well as iridium-catalysed epoxidations of alkenes.<sup>8</sup> Chiral derivatives have been successfully used as stereodirecting ligands in the iron-catalysed hydrosilylation and the cobalt-catalysed cyclopropanation.<sup>9</sup>

Although bpi complexes of many transition metals are known, the derivatives of the 3d metals containing only a single bpi ligand and additional labile ligands, which thus are suitable for catalysis, are often only poorly characterised. This may be due to their substitutional lability and paramagnetism which renders *in situ* characterisation difficult.<sup>10</sup> There have been only a few reports on Co<sup>II</sup> mono(bpi) and Fe<sup>II</sup> mono(bpi) complexes,<sup>5a-c,6a,b,9</sup> and their characterisation by paramagnetic NMR in solution is virtually unexplored. The structural features of, particularly, the iron(II) compounds, recently found to be active hydrosilylation catalysts, remain to be established. Herein we report the synthesis as well as structural and detailed NMR spectroscopic characterisation of iron(II) and cobalt(II) complexes containing bis(2-pyridylimino)isoindolate ligands.

Anorganisch-Chemisches Institut, Universität Heidelberg, Im Neuenheimer Feld 270, 69120, Heidelberg, (Germany). E-mail: lutz.gade@uni-hd.de; Fax: +49-6221-545609

† CCDC reference numbers 821499–821503. For crystallographic data in CIF or other electronic format see DOI: 10.1039/c1dt10617a

## Results and discussion

### Synthesis of the ligand and its lithium salt

Since the syntheses of the desired mono(bpi) complexes using established bpiH derivatives have proved to be cumbersome due to the formation of  $[M(\text{bpi})_2]$  complexes, the sterically more demanding ligand **1** (thqbpiH) was synthesised, for which the formation of “homoleptic” complexes is precluded (Scheme 1). The  $C_{2v}$  symmetry of the ligand facilitates the spectroscopic assignments for the *in situ* characterisation in solution. Moreover, it may be viewed as an achiral analogue to the known chiral ligands featuring similar steric and electronic properties.<sup>9</sup>

ThqbpiH (**1**) was prepared by a modified procedure originally published by Siegl<sup>5a,b</sup> starting from phthalodinitrile and 2-amino-5,6,7,8-tetrahydroquinoline which were refluxed in *n*-hexanol with catalytic amounts of calcium chloride (Scheme 1).<sup>11</sup> The analytical, <sup>1</sup>H and <sup>13</sup>C NMR and the high resolution mass spectrometric data are consistent with the proposed molecular structure, which was further confirmed by X-ray diffraction.

ThqbpiH (**1**) displays approximate molecular  $C_2$  symmetry in the solid state, with the rotational axis passing through the N(1)H bond (Fig. 1). The isoindole backbone is essentially planar, while the tetrahydroquinoline units are tilted by 12.1° and –20.3° out of the molecular plane defined by the isoindole unit. This effect is presumably induced by steric repulsion between the methylene groups C(16)H<sub>2</sub> and C(25)H<sub>2</sub>. Evidently the protonated ligand is already highly pre-organised, which is a favourable feature for metal complexation. The pre-organisation is caused by the delocalized  $\pi$ -electron system, which favours a planar arrangement of the rings, and is further supported by hydrogen bonds formed between the isoindole proton and the pyridine-nitrogen atoms.

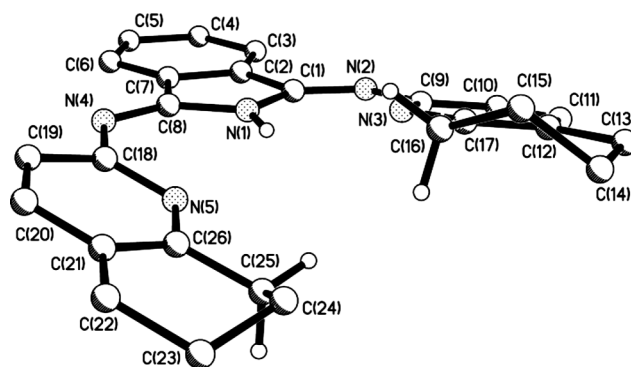
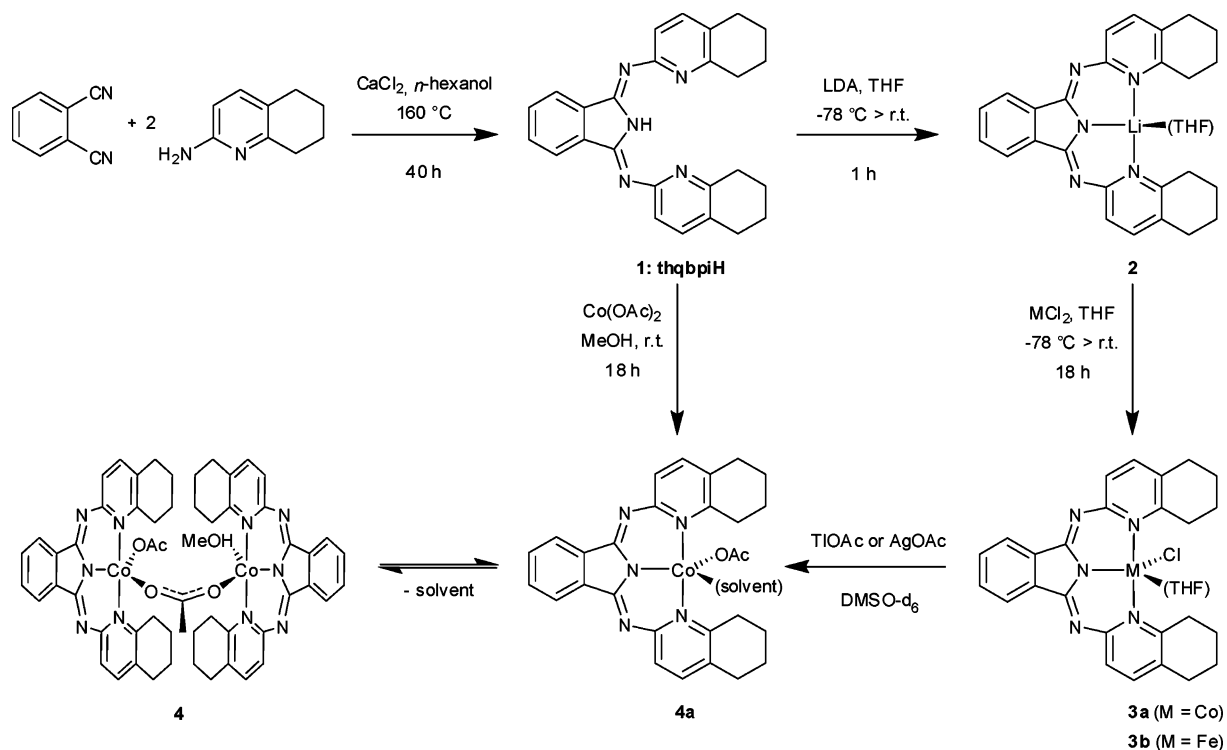


**Fig. 1** Molecular structure of **1**. Hydrogen atoms, except N(1)H, C(16)H<sub>2</sub> and C(25)H<sub>2</sub>, have been omitted for clarity. Selected bond lengths (Å) and angles (°): C(1)–N(1) 1.3877(12), C(1)–N(2) 1.2840(12), C(8)–N(4) 1.2912(12), C(8)–N(1) 1.3867(12), C(9)–N(2) 1.4004(12), C(18)–N(4) 1.4024(12), N(2)–C(1)–N(1) 130.94(8), N(4)–C(8)–N(1) 130.45(8).

Common complexation procedures, based on the direct reaction of the protioligand with different metal salts, which were previously reported for bpi ligands,<sup>5a-c,6a-b</sup> did not readily lead to the formation of the desired mono(bpi) iron(II) or cobalt(II) complexes. Therefore a two step route was used, involving the deprotonation of thqbpiH (**1**) using LDA in THF at –78 °C to yield the corresponding lithium complex **2**. Formation of the lithium complex was monitored by disappearance of the NH signal using NMR spectroscopy. Its formulation and structure were confirmed by high resolution mass spectrometry, elemental analysis and X-ray structure analysis.

Crystals suitable for X-ray diffraction analysis were obtained from a saturated solution of the lithium complex **2** in THF.



**Scheme 1** Preparation of the compounds 1–4.

Substitution of the *NH* proton by a lithium atom forces both tetrahydroquinoline rings into the isoindole plane resulting in reduced interplanar angles (6.1° and 13.2°) and coordination of the metal centre by three nitrogen atoms. Additionally one molecule of THF is found in the coordination sphere, which is best described as distorted tetrahedral. The molecule possesses approximate *C<sub>s</sub>* symmetry neglecting the deviation caused by the flexible cyclohexene subunits of the tetrahydroquinoline moieties (Fig. 2).

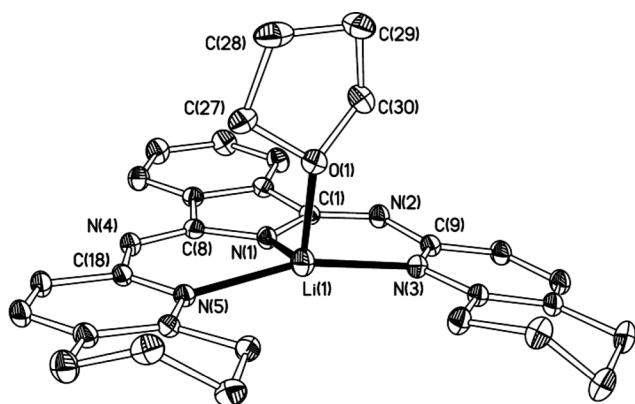


**Fig. 2** Molecular structure of **2**. Hydrogen atoms have been omitted for clarity. Selected bond lengths (Å) and angles (°): N(1)–Li(1) 1.896(2), N(3)–Li(1) 2.125(2), N(5)–Li(1) 2.137(2), O(1)–Li(1) 2.049(2), N(1)–C(1) 1.3699(14), N(2)–C(1) 1.3034(14), N(2)–C(9) 1.3920(14), N(1)–Li(1)–O(1) 112.58(11), O(1)–Li(1)–N(3) 97.36(9), O(1)–Li(1)–N(5) 98.97(9), N(3)–Li(1)–N(5) 162.37(12).

### Synthesis and structural characterisation of the cobalt(II) and iron(II) complexes

Reaction of cobalt(II) chloride or iron(II) chloride with one equivalent of the lithium complex **2** in THF led to formation of the metal complexes **3a** and **3b** (Scheme 1). Their formulation as depicted in Scheme 1 was confirmed by the observation of the molecular ion peaks  $[M+H]^+$  and  $[M-Cl]^+$  in their FAB mass

spectra as well as elemental analysis. The structural details of both complexes were established by X-ray diffraction.

Both complexes **3a** and **3b** were crystallised from a saturated solution in DMSO. Their *C<sub>s</sub>*-symmetric molecular structures are almost superimposable with regard to their key features. According to Hoffmann *et al.*<sup>12</sup> the preferred geometry for *d<sup>6</sup>* and *d<sup>7</sup>* high spin pentacoordinate metal complexes is a trigonal bipyramid. The observed distortion of the complex structures is presumably dominated by the steric demand of the rigid bpi ligand, which also disfavours the coordination of an additional ligand to form stable octahedral complexes.

In both cases the aromatic parts of the tetrahydroquinoline units are almost coplanar to the isoindole plane. The angles between the isoindole plane and the pyridine rings are 6.0° and 10.3° in case of the iron complex as well as 3.1° and 11.4° with respect to the cobalt complex and thus within the same order of magnitude as the ones observed in the lithium complex **2**. As expected, the bond between the metal and the anionic nitrogen atom is about 0.17 Å shorter than to the neutral ligating nitrogen atoms. The two remaining coordination sites are occupied by a chloro ligand and a solvent molecule, in this case DMSO. Corresponding bond lengths and angles of both derivatives are similar, keeping the slightly smaller ionic radius of cobalt(II) in mind. The bpi ligand itself is virtually invariant upon substituting cobalt(II) for iron(II) regarding its structural features. For this reason the larger iron atom is forced out of the isoindole plane by 0.2 Å. This also leads to increased distortion of the coordination geometry. The angle between the anionic nitrogen atom and the coordinating solvent molecule in **3b** N(1)–Fe(1)–O(1) of 97.7° is significantly smaller than the corresponding angle N(1)–Co(1)–O(1) in **3a** (106.3°) (Fig. 3).

Since most reactions catalysed by cobalt(II) bpi systems depend on the application of acetato complexes their structures both in the solid state and in solution are of great interest for a mechanistic understanding of the catalytic reaction. Stirring a solution of **1** and cobalt(II) acetate tetrahydrate in methanol yielded the cobalt(II) complex **4**. The acetato complex **4** is alternatively accessible by treatment of **3a** with one equivalent of silver or thallium acetate in DMSO.

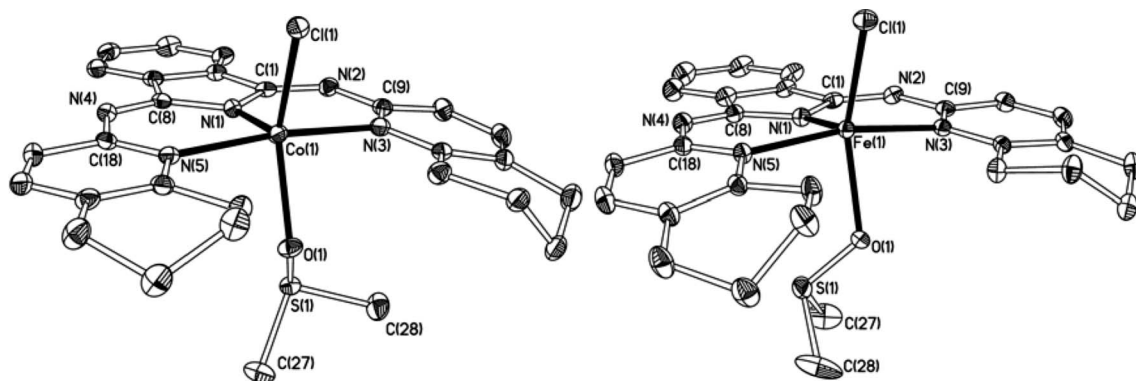


**Fig. 3** Molecular structures of **3a** (left) and **3b** (right). Hydrogen atoms, non-coordinating solvent molecules and disordered atoms have been omitted for clarity. Selected bond lengths (Å) and angles (°) for **3a**: Co(1)–N(1) 1.941(2), Co(1)–O(1) 2.1015(18), Co(1)–N(5) 2.148(2), Co(1)–N(3) 2.173(2), Co(1)–Cl(1) 2.3327(11), N(1)–C(1) 1.386(3), N(2)–C(1) 1.292(3), N(1)–Co(1)–O(1) 106.28(8), O(1)–Co(1)–N(3) 87.39(7), N(5)–Co(1)–N(3) 172.98(7), N(1)–Co(1)–Cl(1) 111.54(6), O(1)–Co(1)–Cl(1) 142.13(5); **3b**: Fe(1)–N(1) 1.9955(13), Fe(1)–O(1) 2.1405(12), Fe(1)–N(3) 2.1667(13), Fe(1)–N(5) 2.1718(13), Fe(1)–Cl(1) 2.3407(9), N(1)–C(1) 1.3752(17), N(2)–C(1) 1.2994(18), N(1)–Fe(1)–O(1) 97.65(5), O(1)–Fe(1)–N(3) 83.09(5), N(3)–Fe(1)–N(5) 168.37(4), N(1)–Fe(1)–Cl(1), 112.75(4), O(1)–Fe(1)–Cl(1) 149.51(3).

Whereas the NMR spectroscopic data supported the formulation of **4a** as given in Scheme 1, the FAB mass spectrum only displayed the fragment peak of  $[M-OAc]^+$  as highest  $m/z$  ion peak. X-ray diffraction analysis revealed dinuclear molecules in the solid state. The two cobalt atoms each bear a bpi ligand and are linked by a bridging acetate. Furthermore, one cobalt atom is coordinated by an additional acetato unit, while the second bears a molecule of methanol, which was employed as the solvent for synthesis as well as crystallisation. The observed coordination geometry is approximately distorted trigonal bipyramidal with the angles between the bridging acetato anion and methanol  $[143.39(7)^\circ]$  or the terminal acetato ligand  $[139.19(7)^\circ]$  being opened up. Each metal atom is located within a plane defined by the particular isoindole backbone (Fig. 4).

As anticipated, the bond between the negatively charged isoindolato nitrogen and the cobalt atom (1.94 Å) is 0.21 Å shorter than the average of the pyridine nitrogen atoms (2.15 Å) for both cobalt atoms. The bridging acetato ligand is almost symmetrically bonded to both cobalt atoms (bond lengths Co(1)–O(4) 2.02 and Co(2)–O(3) 2.04 Å), which is also reflected in the equal distance between the carboxyl carbon and both oxygen atoms. In contrast to the only other cobalt-acetato-bpi structure the complex reported in the literature does not crystallise in a polymeric form.<sup>5f</sup> This is probably caused by the steric demand of this pincer ligand. Nevertheless this complex is only sparingly soluble in organic solvents with the exception of methanol and DMSO.

## Paramagnetic NMR spectroscopy of the iron and cobalt complexes

For all complexes paramagnetic  $^1H$  as well as  $^{13}C$  NMR spectra were recorded at variable temperatures. The cobalt(II) complexes give rise to well resolved paramagnetic NMR spectra. Due to the rapid electron relaxation of the high spin  $d^7$  or  $d^6$  systems relatively sharp resonances are expected.<sup>13</sup> At 295 K line widths in the  $^1H$  NMR in the range of 200 to 490 Hz for the iron system and 100 to 600 Hz for the cobalt complexes are observed.

The theory of the unpaired electron-nucleus interaction and its consequences for NMR spectroscopy has been developed over the past decades and has been summarised comprehensively.<sup>13</sup> In diamagnetic molecules the orbital shift ( $\delta_{orb}$ ) provides the principal contribution to the observed chemical shifts. In paramagnetic samples the temperature dependent hyperfine shift ( $\delta_{hf}$ ) adds to the orbital shift, leading to the observed chemical shift:

$$\delta_{obs} = \delta_{orb} + \delta_{hf} \quad (1)$$

The hyperfine shift itself may be expressed as stated in eqn (2), where  $S$  is the total electron spin,  $\beta_e$  the Bohr magneton,  $\gamma_N$  the nuclear gyromagnetic ratio, finally  $g$  and  $A$  are the  $g$ - and  $A$ -hyperfine tensors.

$$\delta_{hf} = \frac{S(S+1)\beta_e}{3kT\gamma_N} gA \quad (2)$$

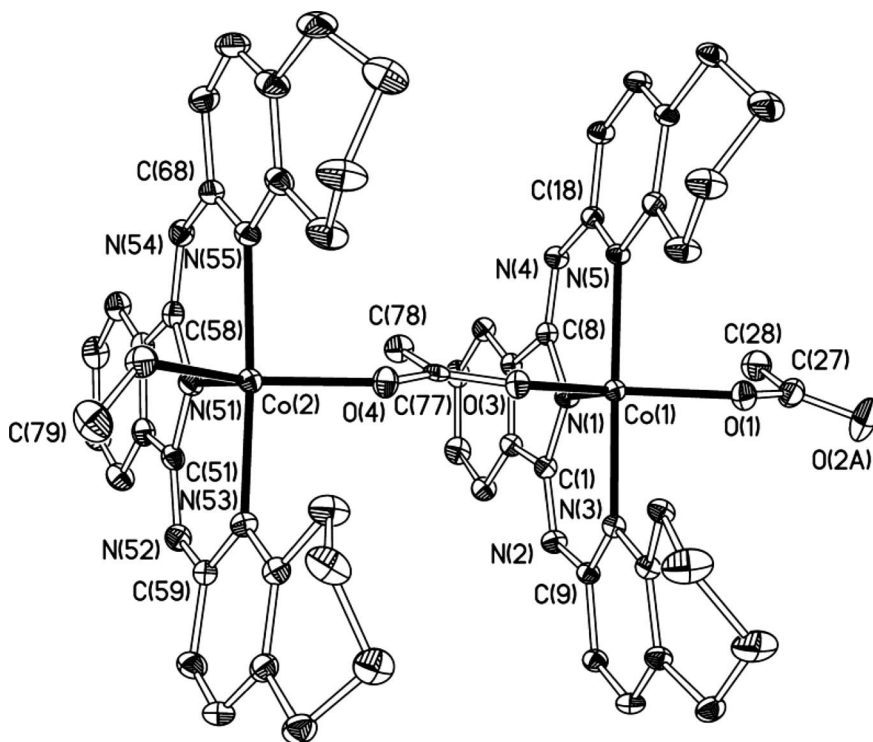


**Fig. 4** Molecular structure of **4**. Hydrogen atoms, non-coordinating solvent molecules and disordered atoms have been omitted for clarity. Selected bond lengths (Å) and angles ( $^\circ$ ): Co(1)–N(1) 1.9405(19), Co(1)–O(3) 2.0378(18), Co(1)–O(1) 2.0412(19), Co(1)–N(3) 2.141(2), Co(1)–N(5) 2.1628(19), C(77)–O(3) 1.256(3), C(77)–O(4) 1.262(3), Co(2)–N(51) 1.939(2), Co(2)–O(4) 2.0188(19), Co(2)–O(5) 2.0774(18), Co(2)–N(53) 2.119(2), Co(2)–N(55) 2.171(2), N(1)–Co(1)–O(3) 109.64(7), O(3)–Co(1)–O(1) 139.19(7), N(1)–Co(1)–N(3) 90.22(8), O(3)–Co(1)–N(3) 89.57(7), N(1)–Co(1)–N(5) 89.84(8), O(1)–Co(1)–N(5) 90.64(7), N(3)–Co(1)–N(5) 178.77(7), N(51)–Co(2)–O(4) 112.37(7), O(4)–Co(2)–O(5) 143.39(7), N(51)–Co(2)–N(53) 91.37(8), O(4)–Co(2)–N(53) 92.16(7), N(51)–Co(2)–N(55) 89.27(8), O(5)–Co(2)–N(55) 83.06(7), N(53)–Co(2)–N(55) 175.78(7).

For an arbitrary number of unpaired electrons a general expression of the NMR shielding tensor has been developed only recently.<sup>14a</sup> Although there are several isotropic and anisotropic contributions to  $\delta_{hf}$ , it is possible to analyse paramagnetic NMR spectra in solution by considering only three contributions, namely the orbital shift ( $\delta_{orb}$ ), the Fermi contact shift ( $\delta_{con}$ ) and the pseudocontact shift ( $\delta_{pc}$ ). Consequently eqn (1) may be simplified to eqn (3):

$$\delta_{obs} = \delta_{orb} + \delta_{hf} \cong \delta_{orb} + \delta_{con} + \delta_{pc} \quad (3)$$

The Fermi contact shift is caused by coupling of the unpaired electrons with the atomic nuclei and is transmitted through chemical bonds.  $\delta_{con}$  is proportional to the residual spin density at the atom centre ( $\rho_{\alpha\beta}$ ). The latter can be extracted from DFT calculations so that  $\delta_{con}$  can be obtained by using eqn (4):

$$\delta_{con} = \frac{\mu_0 \mu_B^2 g_c^2}{9k} \cdot \frac{(S+1)}{T} \rho_{\alpha\beta} \quad (4)$$

The pseudocontact shift arises from a dipolar through-space interaction between the magnetic moment of unpaired electrons and the magnetic moments of the nuclei. It depends strongly on the distance of the examined nucleus to the paramagnetic centre and may be of little influence to the chemical shift of nuclei distant from the metal core. Thus the Fermi contact is presumed to dominate the chemical shifts of covalently bound ligands in 3d metal complexes.<sup>15,16</sup>

In order to allow the assignment of the paramagnetic NMR spectra, DFT calculations were performed using the B3LYP<sup>17</sup> functional and employing a TZVP<sup>18</sup> basis set for the metal atoms as well as a 6-311G(d,p) basis set for all other atoms.<sup>19</sup> This approach reliably predicts hyperfine shifts as has been shown recently.<sup>14-16</sup> The computed spin densities were employed to calculate the hyperfine shifts caused by the Fermi contact interaction using eqn (4). The chemical shifts of the protio ligand **1** were used to determine the experimental orbital terms. These values deviate only slightly from the chemical shifts of the lithium complex **2**, which may also serve as diamagnetic model.

The use of a cryogenically cooled <sup>13</sup>C detection probe and optimised repetition times allowed recording of paramagnetic <sup>13</sup>C NMR spectra within a few minutes. The assignment of the carbon resonances is based upon a series of <sup>13</sup>C NMR experiments with selective <sup>1</sup>H-decoupling, correlation experiments and DFT calculations.

The cobalt(II) chloro complex **3a** displays eleven proton resonances at 295 K which arise from eleven of the twelve non-equivalent H atoms of a *C<sub>s</sub>*-symmetric molecule as depicted in Fig. 5. One signal was not detected, presumably due to its close vicinity to the paramagnetic metal centre and a resulting substantial dipolar relaxation (*r*<sup>-6</sup> dependence).<sup>13</sup>

Four resonances can be easily assigned to aromatic protons, as a <sup>13</sup>C-<sup>1</sup>H correlation experiment shows their direct connection to carbon atoms, which give rise to doublets in the <sup>1</sup>H-coupled <sup>13</sup>C NMR spectra (Fig. 6). These signals display Curie behaviour with increased temperature, while the seven resonances of the aliphatic protons start to broaden. Coalescence is reached between 330 and 340 K. Above that temperature four averaged signals were detected. No signals of coordinating solvent molecules were detectable.

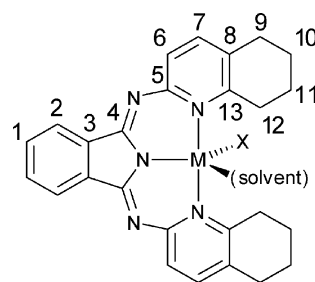


Fig. 5 Labelling of the atoms used in discussion of the paramagnetic NMR spectra.

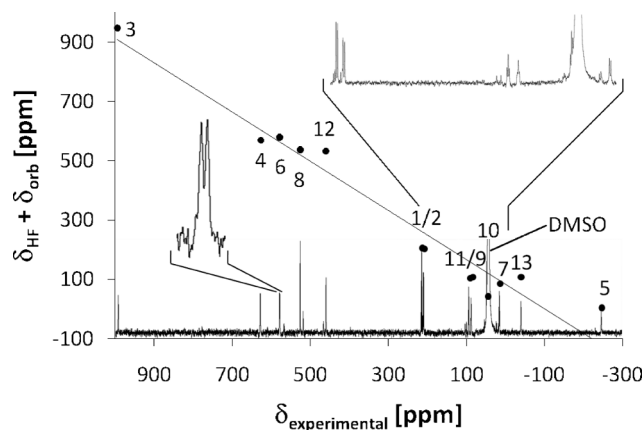


Fig. 6 Plot of the measured paramagnetic <sup>13</sup>C NMR chemical shift against the corresponding sum of the calculated hyperfine shift and the orbital contribution for all carbon atoms of **3a**; the approximate linear relation was used to assign the resonances. The expanded sections of the spectrum illustrate the multiplicity of some of the signals. (295 K, 600 MHz, DMSO-*d*<sub>6</sub>). For the numbering of the <sup>13</sup>C-nuclei, see Fig. 5.

As expected for the *C<sub>s</sub>*-symmetric complex 13 signals are observed in the <sup>13</sup>C NMR spectrum in the range of -250 to 1000 ppm. The aromatic carbons can be identified by their <sup>1</sup>J<sub>CH</sub>-coupling to one proton giving rise to doublets in the <sup>1</sup>H-coupled spectra. Analogously, the CH<sub>2</sub> carbon atoms appear as triplets. Secondary and tertiary carbon atoms were assigned to the corresponding protons by correlation experiments, whilst the remaining quaternary <sup>13</sup>C nuclei give rise to signals without <sup>1</sup>J<sub>CH</sub>-coupling to protons.

Unpaired electrons of the cobalt core are delocalised into molecular orbitals also located on the ligand. This is reflected in large calculated values for the spin density at certain atoms of the bpi system.<sup>20</sup> The highest values are predicted for the C3 and C4 atoms, which are part of the isoindole-subunit (Fig. 6). Likewise the pyridine carbon atoms also bear a high amount of spin density. The atoms C5, C7 and C13, which are connected to the cobalt core by an even number of bonds, show negative Fermi contact contributions, while C6 and C8 exhibit positive values and are linked to the metal centre by an odd number of bonds. The aromatic carbon atoms C1 and C2 are only slightly influenced by the unpaired electrons. Within the aliphatic carbon atoms (C9–C12) C12 is separated from the Co atom by the smallest number of bonds and consequently bears the highest spin density.

The calculated carbon shifts are in good agreement with the observed chemical shifts and enable a reasonable assignment of the resonances. However, some of the theoretically determined proton

shifts deviate from the measured values. This discrepancy may be caused by a fast ring inversion in the cyclohexene unit. Whereas the calculated spin-densities are based on a single energy minimum of the fluxional molecule, the experimental NMR values are a result of several conformational contributions. Coordination or decoordination of the coordinating solvent molecule dramatically influences the calculated proton shifts and leads to a much worse correlation with the observed  $^1\text{H}$  NMR spectrum. Although the lability of coordinating solvent molecules is already known for similar cobalt(II) bpi complexes the NMR spectra are not in accordance with a significant contribution of a fourfold coordinated species in solution.<sup>5f</sup>

The isostructural iron(II) complex **3b** displays similar behaviour to **3a**. For four resonances of the aromatic protons a normal, Curie-type temperature dependence was observed. These signals are assigned according to their computed spin densities. Compared to the protons of the pyridine rings, the isoindole protons carry only small spin densities and thus give rise to signals with only small paramagnetic shifts. The two protons of the pyridine units are shifted more strongly, as they are closer to the paramagnetic centre. Of the eight aliphatic protons only six are detectable at 295 K. All of these signals show coalescence at about 320 K (Fig. 7). Again these signals are assigned according to their computed spin densities, which are decreasing with the number of bonds to the paramagnetic centre. The proton signals of the  $\text{CH}_2$ -group 12 are not detectable, presumably due to a strong dipolar interaction with the spatial close iron core. Additionally there is one equivalent of uncoordinated THF present, which was substituted by the solvent  $\text{DMSO-d}_6$ .

As anticipated the cobalt acetato complex **4a** shows a  $^1\text{H}$  NMR spectrum similar to the one of the chloro complex **3a** with almost identical chemical shifts. The coalescence temperature of the dynamic behaviour for this compound is observed at about 310 K. An additional signal can be found at 39.27 ppm which may be assigned to the acetato group.

In the  $^{13}\text{C}$  NMR spectra all of these metal complexes display Curie behaviour in solution over the studied temperature range of 290 to 340 K. The Curie plot of the proton chemical shifts illustrates the observed dynamic behaviour and shows the expected linear correlation between chemical shifts and inverse temperature (Fig. 7). Spectrometer and solvent limitations prohibited the examination of a broader temperature interval.

Finally, the paramagnetic susceptibility of the chloro complexes in solution was measured by the Evans method.<sup>21</sup> The magnetic moment of **3a** is comparable to that of previously reported high spin cobalt(II) bpi complexes<sup>10c</sup> ( $\mu_{\text{eff}} = 4.17 \mu_{\text{B}}$ ) and the one of **3b** is in the range of high spin iron(II) bpi complexes ( $\mu_{\text{eff}} = 5.57 \mu_{\text{B}}$ ).<sup>4a</sup> The rather large value of the iron complex may be attributed to pronounced spin orbit coupling, which is commonly observed for distorted iron(II) complexes.<sup>22</sup>

#### Analysis of the dynamic behaviour

The  $^1\text{H}$  NMR spectra of **3a** and **3b** display dynamic behaviour of some resonances of the complexes at temperatures above 300 K. The corresponding pairs of signals of the diastereotopic  $\text{CH}_2$  proton atoms show broadening, coalescence and collapse to singlets. The other NMR signals are not affected by varying the

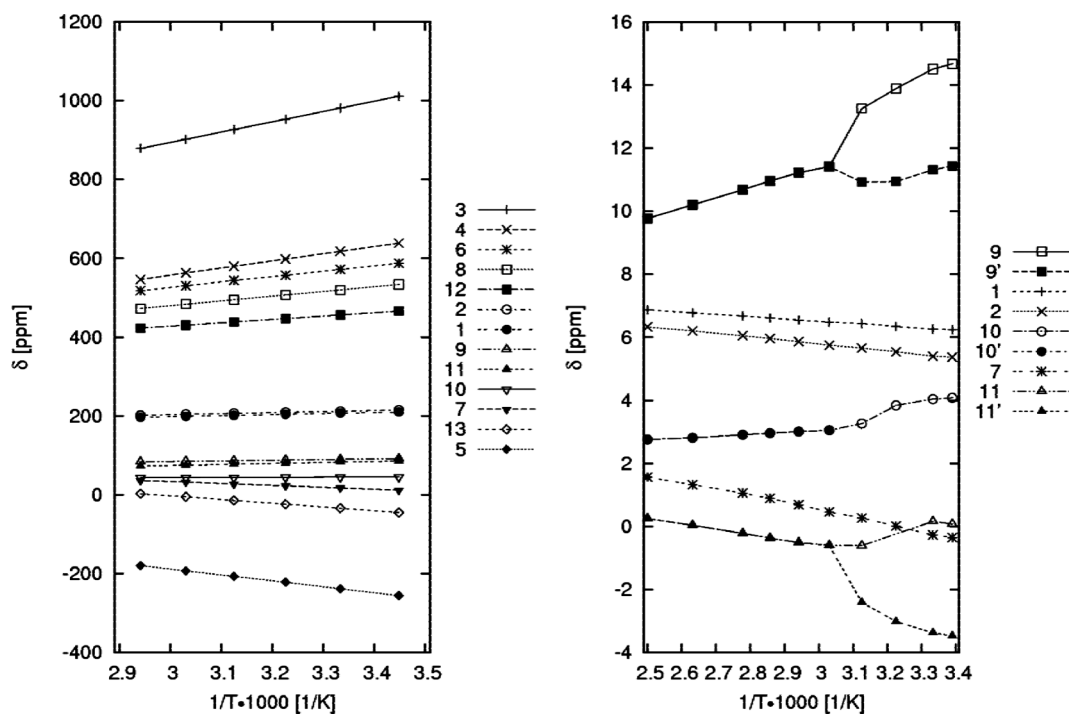


**Fig. 7** Curie plot showing the linear dependence of  $^{13}\text{C}$  resonance shifts on the inverse temperature for **3a** (left). The  $^1\text{H}$  spectra of **3b** (right) display Curie behaviour in the fast and slow exchange region and a deviation close to coalescence temperature caused by “pseudorotation” of the Cl-M-DMSO unit. (The signal of H10' is superposed by the solvent signal at lower temperatures.)

temperature (apart from the Curie shift and typical line shape variations due to temperature dependent relaxation behaviour). Considering a fast cyclohexene ring inversion, each CH<sub>2</sub> group has one H atom pointing to the same side of the molecular plane as the chloro ligand and the other H atom to the side of the coordinated solvent molecule. Interconversion of the diastereotopic positions has to occur along with a pseudo-rotation of the Cl-M-solvent moiety. An exchange of this type can be realised either by dissociation of the solvent or by an associative mechanism in which a second dimethylsulfoxide molecule enters the coordination sphere to form a sixfold coordinated transition state (or high energy intermediate). We have performed line shape analysis of the dynamic <sup>1</sup>H NMR spectra (Fig. 8) in order to extract activation entropies from the temperature dependence of the activation Gibbs energies ( $\Delta G^\ddagger$ ). For modelling the line shape behaviour of a two-site exchange only three parameters are necessary: the chemical shifts of the exchanging signal pairs at various temperatures, the line width in the absence of exchange and the exchange rate itself. The temperature dependent shifts of the signal pairs in and above the coalescence region were calculated by linear extrapolation against T<sup>-1</sup> (Curie behaviour).

The line shape was derived from a similar non-exchanging signal so that the exchange rates as the third parameters could be extracted. Extrapolation within an Eyring plot leads to strongly negative activation entropies ( $\Delta S^\ddagger = -154 \pm 25 \text{ J mol}^{-1} \text{ K}^{-1}$  for **3a** and  $\Delta S^\ddagger = -168 \pm 15 \text{ J mol}^{-1} \text{ K}^{-1}$  for **3b**). These values are in accordance with an associative exchange mechanism for the rearrangement of the Cl-M-DMSO unit through a

sixfold coordinated transition state or high energy intermediate (Scheme 2).

## Conclusions

A reliable and convenient synthetic route to mono-bpi cobalt(II) and iron(II) complexes has been developed, and for the first time iron complexes of this type, having gained considerable importance in catalysis,<sup>9</sup> have been structurally characterised. Moreover the structural features of all metal complexes in solution have been determined using paramagnetic NMR spectroscopy in combination with computational methods. These data support some of the previous proposals about the structure of mono-bpi metal complexes and provide new insight into their geometry and their dynamic behaviour. The analysis of the paramagnetic and dynamic NMR spectra shows that associative exchange mechanisms are operative which is a valuable information for the understanding of catalytic processes with such systems. Based on these results the methods employed in this work appear to be suitable for the *in situ* characterisation of the structurally more complicated chiral derivatives.<sup>9</sup>

## Experimental

### General experimental procedures

All manipulations of air and moisture-sensitive materials were performed under an inert atmosphere of dry argon using standard

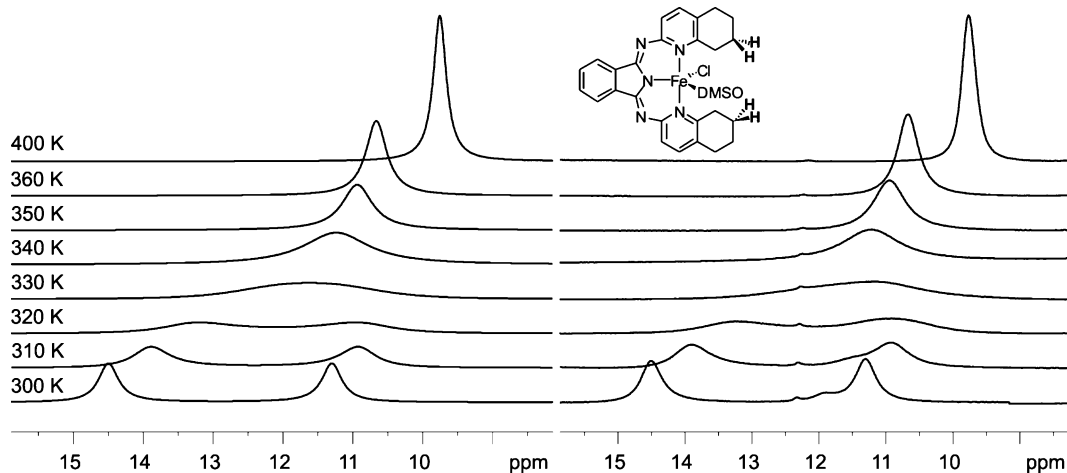
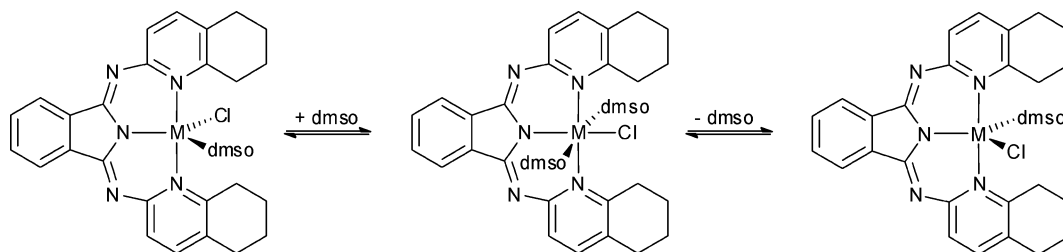


**Fig. 8** Results of the line shape analysis of **3b**. Section corresponding to CH<sub>2</sub>(11) of the experimental spectrum (right) compared to the simulated one (left).



**Scheme 2** Inversion on the metal centre *via* associative mechanism. On the NMR-timescale rapid coordination and elimination of a second DMSO molecule leads to averaged signals of the diastereotopic protons.

Schlenk techniques. Solvents were purified and dried by standard methods. 2-(2-Cyanoethyl)cyclohexanone oxime<sup>23</sup> was synthesised according to reported procedures. All other reagents were obtained commercially and used as received. <sup>1</sup>H and <sup>13</sup>C spectra were recorded on Bruker Avance II 400 and Bruker Avance III 600 NMR spectrometers and were referenced using the residual protio solvent (<sup>1</sup>H) or solvent (<sup>13</sup>C) resonances. The paramagnetic <sup>13</sup>C NMR spectra were measured with a Bruker QNP Cryo Probe. Mass spectrometry and elemental analyses were obtained by the analytical service of the Heidelberg Chemistry Department.

### Preparation of the compounds

**2-Amino-5,6,7,8-tetrahydroquinoline.** In a round bottom flask equipped with a condenser 2-(2-cyanoethyl)cyclohexanone oxime (56.1 g, 338 mmol) was dissolved in acetic anhydride (57 ml, 506 mmol) while being cooled using an ice bath. Acetyl chloride (59 ml, 676 mmol) was added and the red solution was refluxed for 16 h. The resulting mixture was neutralised with saturated, aqueous sodium bicarbonate and extracted four times with dichloromethane (300 ml). The combined organic layers were concentrated in a rotary evaporator to yield crude 2-(*N*-acetylamino)-5,6,7,8-tetrahydroquinoline as an orange solid, which was used without further purification in the next step. After addition of NaOH (85.0 g, 2125 mmol) in water (350 ml), the resulting mixture was refluxed for three hours. The obtained solution was extracted three times with dichloromethane (500 ml). (Phase separation occurs only very slowly.) The combined organic phases were dried over Na<sub>2</sub>SO<sub>4</sub> and concentrated in a rotary evaporator. The crude product was purified using flash column chromatography (SiO<sub>2</sub>, Et<sub>2</sub>O/NEt<sub>3</sub> = 97:3, R<sub>f</sub> 0.2) to yield 2-amino-5,6,7,8-tetrahydroquinoline as an orange, crystalline solid (9.4 g, 20% over two steps). The recorded spectroscopic data are in good agreement with the reported data.<sup>23</sup> Found: C, 72.4; H, 8.2; N, 18.4. Calc. for C<sub>9</sub>H<sub>12</sub>N<sub>2</sub>: C, 72.9; H, 8.2; N 18.9.

**ThqbpH (1).** A suspension of phthalodinitrile (3.3 g, 26 mmol), 2-amino-5,6,7,8-tetrahydroquinoline (9.0 g, 60 mmol) and CaCl<sub>2</sub> (0.3 g, 3 mmol) in *n*-hexanol (100 ml) was refluxed at 160 °C for 40 h. After cooling to room temperature, hexanol was removed *in vacuo*. The resulting black solid was dissolved in dichloromethane, filtered over celite and concentrated in a rotary evaporator. The crude product was recrystallised from EtOH/MeOH = 1:1 to yield **1** as yellow crystals (8.6 g, 81%). Crystals suitable for an X-ray diffraction study were obtained from a saturated solution of **1** in CH<sub>2</sub>Cl<sub>2</sub>. Found: C, 76.1; H, 6.2; N, 16.95; Calc. for C<sub>26</sub>H<sub>25</sub>N<sub>5</sub>: C, 76.6; H, 6.2; N, 17.2. <sup>1</sup>H NMR (600 MHz, CD<sub>2</sub>Cl<sub>2</sub>, 295 K) δ 12.37 (s, 1H, NH), 7.99–7.06 (m, 2H, H1), 7.64–7.61 (m, 2H, H2), 7.41 (d, <sup>3</sup>J = 8.3 Hz, 2H, H6), 7.05 (d, <sup>3</sup>J = 8.3 Hz, 2H, H5), 2.81 (t, <sup>3</sup>J = 6.4 Hz, 4H, H12), 2.76 (t, <sup>3</sup>J = 6.4 Hz, 4H, H9), 1.89–1.85 (m, 4H, H11), 1.83–1.79 (m, 4H, H10). <sup>13</sup>C {<sup>1</sup>H} NMR (150 MHz, CD<sub>2</sub>Cl<sub>2</sub>, 295 K) δ 158.5 (C5), 156.1 (C13), 152.7 (C4), 139.4 (C7), 136.3 (C3), 132.0 (C1), 129.3 (C8), 122.7 (C2), 119.4 (C6), 33.6 (C12), 28.9 (C9), 23.6 (C11), 23.4 (C10). HR-MS (ESI+) *m/z* (%): Calc. for C<sub>26</sub>H<sub>26</sub>N<sub>5</sub><sup>+</sup> ([M+H]<sup>+</sup>): 408.2183; Found: 408.2184 (100).

**[Li(THF)(thqbp)] (2).** A solution of LDA (58 mg, 0.55 mmol) in THF (4 ml) was added to a solution of thqbpH (204 mg, 0.50 mmol) in THF (10 ml) at –78 °C. The cooling bath was removed

and the reaction mixture was stirred for 45 min. THF was removed *in vacuo*. The remaining solid was washed with hexane to yield [Li(thqbp)] (**2**) as a yellow solid (230 mg, 98%). Crystals suitable for an X-ray diffraction study were obtained by slow diffusion of hexane into a saturated solution of **2** in THF. Found: C, 75.6; H, 6.2; N, 16.9. Calc. for C<sub>26</sub>H<sub>24</sub>LiN<sub>5</sub>: C, 75.5; H, 5.85; N, 16.9. <sup>1</sup>H NMR (600 MHz, THF-d<sub>8</sub>, 295 K) δ 7.88–7.87 (m, 2H, H1), 7.45–7.44 (m, 2H, H2), 7.44 (d, <sup>3</sup>J = 7.8 Hz, 2H, H6), 7.22 (d, <sup>3</sup>J = 7.8 Hz, 2H, H5), 3.12 (t, <sup>3</sup>J = 6.2 Hz, 4H, H10), 2.82 (t, <sup>3</sup>J = 6.2 Hz, 4H, H9), 2.06–2.02 (m, 4H, H11), 1.93–1.89 (m, 4H, H10). <sup>13</sup>C {<sup>1</sup>H} NMR (150 MHz, THF-d<sub>8</sub>, 295 K) δ 167.9 (C5), 161.8 (C13), 154.8 (C4), 143.6 (C7), 140.0 (C3), 130.2 (C1), 126.7 (C8), 124.4 (C2), 122.4 (C6), 35.3 (C12), 29.7 (C9), 24.8 (C11), 24.4 (C10). <sup>7</sup>Li {<sup>1</sup>H} NMR (155 MHz, THF-d<sub>8</sub>, 295 K) δ 2.13. HR-MS (FAB+) *m/z* (%): Calc. for C<sub>26</sub>H<sub>25</sub>LiN<sub>5</sub><sup>+</sup> ([M+H]<sup>+</sup>) 414.2270; Found 414.2228 (100).

**[CoCl(THF)(thqbp)] (3a).** A solution of LDA (28.9 mg, 0.27 mmol) in THF (3 ml) was added to a solution of the ligand (100 mg, 0.25 mmol) in THF (5 ml) at –78 °C. After the addition was completed the solution was warmed to room temperature and stirred for another 30 min. Then a solution of CoCl<sub>2</sub>·THF (58.1 mg, 0.27 mmol) in THF (4 ml) was added dropwise *via* cannula. The solution was stirred at room temperature for 18 h. Then the solvent was filtered off and dried *in vacuo*. After subsequent washing with THF the desired product was obtained as a dark green powder (99 mg, 80%). Crystals suitable for an X-ray diffraction study were obtained from a saturated solution of **3a** in DMSO. Found: C, 57.3; H, 5.1; N, 11.8. Calc. for C<sub>28</sub>H<sub>30</sub>ClCoN<sub>5</sub>O: C, 57.1; H, 5.2; N, 12.1. <sup>1</sup>H NMR (600 MHz, DMSO-d<sub>6</sub>, 295 K, paramagnetic) δ 12.1 (2H, H6), 11.0 (2H, H1), 9.8 (2H, H9), 8.1 (2H, H9'), 7.9 (2H, H2), –3.2 (2H, H7), –4.4 (2H, H10), –5.4 (2H, H11), –5.6 (2H, H10'), –8.2 (2H, H11'), –42.9 (2H, H12); The second resonance of H12 is not detected. <sup>13</sup>C {<sup>1</sup>H} NMR (150 MHz, DMSO-d<sub>6</sub>, 295 K, paramagnetic) δ 994.6 (C3), 627.0 (C4), 578.8 (C6), 526.1 (C8), 460.7 (C12), 213.3 (C1), 208.3 (C2), 90.8 (C11), 84.0 (C9), 45.0 (C10), 14.7 (C7), –39.0 (C13), –245.9 (C5). HR-MS (FAB+) *m/z* (%): Calc. for C<sub>26</sub>H<sub>25</sub>ClCoN<sub>5</sub><sup>+</sup> ([M+H]<sup>+</sup>) 501.1131; Found 501.1135 (32); Calc. for C<sub>26</sub>H<sub>24</sub>CoN<sub>5</sub><sup>+</sup> ([M–Cl]<sup>+</sup>) 465.1364; Found 465.1340 (100). Magnetic susceptibility in DMSO-d<sub>6</sub> (295 K): μ = 4.17 μ<sub>B</sub>.

**[FeCl(THF)(thqbp)] (3b).** A solution of LDA (290 mg, 2.75 mmol) in THF (20 ml) was added to a solution of thqbpH (1020 mg, 2.50 mmol) in THF (75 ml) at –78 °C. The cooling bath was removed and the yellow solution was stirred for 60 min. Subsequently the yellow reaction mixture was transferred to a suspension of anhydrous FeCl<sub>2</sub> (350 mg, 2.75 mmol) in THF (75 ml). The reaction mixture was stirred at room temperature for 18 h. The precipitating brown solid was filtered off, washed with THF (10 ml) and dried *in vacuo* to yield [FeCl(THF)(thqbp)] (**3b**) as a brown solid (1060 mg, 74%). Crystals suitable for an X-ray diffraction study were obtained from a saturated solution of **3b** in DMSO. Found: C, 63.2; H, 5.6; N, 12.4. Calc. for C<sub>30</sub>H<sub>32</sub>ClFeN<sub>5</sub>O: C, 63.2; H, 5.7; N, 12.3. <sup>1</sup>H NMR (600 MHz, DMSO-d<sub>6</sub>, 295 K, paramagnetic) δ 41.7 (2H, H6), 14.7 (2H, H9), 11.4 (2H, H9'), 6.2 (2H, H1), 5.4 (2H, H2), 4.1 (2H, H10), 0.1 (2H, H11), –0.35 (2H, H7), –3.5 (2H, H11'); The second resonance of H10 is superposed by the solvent signal, while H12 are not detected. <sup>13</sup>C {<sup>1</sup>H} NMR

**Table 1** Details of the crystal structure determinations of **1**, **2**, **3a**, **3b** and **4**

Compound	<b>1</b>	<b>2</b>	<b>3a</b>	<b>3b-DMSO</b>	<b>4-1.54 MeOH</b>
Formula	C <sub>26</sub> H <sub>25</sub> N <sub>5</sub>	C <sub>30</sub> H <sub>32</sub> LiN <sub>5</sub> O	C <sub>28</sub> H <sub>30</sub> ClCoN <sub>5</sub> OS	C <sub>30</sub> H <sub>36</sub> ClFeN <sub>5</sub> O <sub>2</sub> S <sub>2</sub>	C <sub>38.53</sub> H <sub>64.15</sub> Co <sub>2</sub> N <sub>10</sub> O <sub>6.53</sub>
<i>M<sub>r</sub></i>	407.51	485.55	579.01	654.06	1129.91
Crystal system	Monoclinic	Monoclinic	Orthorhombic	Monoclinic	Monoclinic
Space group	<i>P</i> 2 <sub>1</sub> / <i>n</i>	<i>P</i> 2 <sub>1</sub> / <i>n</i>	<i>P</i> <i>c</i> <i>a</i> 2 <sub>1</sub>	<i>P</i> 2 <sub>1</sub> / <i>c</i>	<i>P</i> 2 <sub>1</sub> / <i>c</i>
<i>a</i> /Å	11.864(5)	11.194(5)	16.954(9)	8.838(4)	13.578(7)
<i>b</i> /Å	15.282(6)	18.995(9)	8.904(5)	16.324(7)	14.502(7)
<i>c</i> /Å	12.121(5)	11.738(6)	17.198(8)	20.602(9)	26.573(15)
$\beta$ (°)	111.42(1)	90.69(1)		90.21(2)	100.720(7)
<i>V</i> /Å <sup>3</sup>	2046(2)	2496(2)	2596(2)	2972(2)	5141(5)
<i>Z</i>	4	4	4	4	4
<i>F</i> <sub>000</sub>	864	1032	1204	1368	2366
<i>d<sub>c</sub></i> /Mg m <sup>-3</sup>	1.323	1.292	1.481	1.462	1.460
$\mu$ (Mo-K $\alpha$ )/mm <sup>-1</sup>	0.081	0.080	0.877	0.776	0.711
max., min. transmission factors	0.8623, 0.8196	0.8623, 0.7964	0.7464, 0.6923	0.9791, 0.8147	0.7464, 0.6560
$\theta$ range/°	2.1 to 31.5	2.0 to 32.3	2.3 to 30.5	1.99 to 32.3	1.97 to 31.50
Index ranges (indep. set) <i>h,k,l</i>	-17...16, 0...22, 0...17	-16...16, 0...28, 0...17	0...24, 0...12, -24...24	-13...13, 0...24, 0...30	-19...19, 0...21, 0...39
Reflections measured	51391	63099	63380	75048	127398
unique [ <i>R</i> <sub>int</sub> ]	6741 [0.0329]	8437 [0.0428]	7944 [0.0864]	10075 [0.0426]	16947 [0.0735]
observed [ <i>I</i> ≥ 2 $\sigma$ ( <i>I</i> )]	5732	6541	6622	8279	11952
Parameters refined	356	430	336	412	790
Goof on <i>F</i> <sup>2</sup>	1.058	1.059	1.037	1.041	1.034
<i>R</i> indices [ <i>F</i> > 4 $\sigma$ ( <i>F</i> )] <i>R</i> ( <i>F</i> ), <i>wR</i> ( <i>F</i> <sup>2</sup> )	0.0433, 0.1130	0.0492, 0.1314	0.0388, 0.0672	0.0359, 0.0862	0.0547, 0.1136
<i>R</i> indices (all data) <i>R</i> ( <i>F</i> ), <i>wR</i> ( <i>F</i> <sup>2</sup> )	0.0529, 0.1246	0.0675, 0.1445	0.0571, 0.0725	0.0495, 0.0930	0.0918, 0.1280
absolute structure parameter			0.009(11)		
largest residual peaks/e-Å <sup>-3</sup>	0.511, -0.262	0.540, -0.248	0.495, -0.418	0.844, -0.514	0.980, -0.925

(150 MHz, DMSO-*d*<sub>6</sub>, 295 K, paramagnetic)  $\delta$  848.6 (C3), 686.9 (C12), 514.5 (C4), 418.2 (C6), 382.7 (C8), 204.2 (C1), 200.8 (C2), 179.2 (C7), 117.2 (C9), 94.7 (C11), 51.9 (C10), -72.4 (C5/13). HR-MS (FAB+) *m/z* (%): Calc. for C<sub>26</sub>H<sub>25</sub>ClFeN<sub>5</sub><sup>+</sup> ([M+H]<sup>+</sup>) 498.1142; Found 498.1120 (29); Calc. for C<sub>26</sub>H<sub>24</sub>FeN<sub>5</sub><sup>+</sup> ([M-Cl]<sup>+</sup>) 462.1376; Found 462.1338 (23). Magnetic susceptibility in DMSO-*d*<sub>6</sub> (295 K):  $\mu = 5.57 \mu_B$ .

**[{Co(OAc)(thqbp)}<sub>2</sub>(MeOH)] (4)**. ThqbpH (100 mg, 0.25 mmol) was added to a solution of Co(OAc)<sub>2</sub>·4 H<sub>2</sub>O in methanol and stirred for 18 h at room temperature. The precipitate was filtered off, washed with THF, and dried *in vacuo* to yield [{Co(OAc)(thqbp)}<sub>2</sub>(MeOH)] as an orange powder (105 mg, 80%). Crystals suitable for an X-ray diffraction study were obtained from a saturated solution of **4** in methanol. Found: C, 59.9; H, 5.1; N, 11.9. Calc. for C<sub>30</sub>H<sub>33</sub>CoN<sub>5</sub>O<sub>3</sub>S: C, 59.8; H, 5.5; N, 11.6. <sup>1</sup>H NMR (600 MHz, DMSO-*d*<sub>6</sub>, 295 K, paramagnetic)  $\delta$  39.3 (OAc), 14.1 (H6), 11.9 (H1), 10.9 (H9), 10.1 (H2), 8.7 (H9'), -1.7 (H7), -3.0 (H10), -4.8 (H11), -35.8 (H12); The second resonances of H10, H11, and H12 are not detected. <sup>13</sup>C {<sup>1</sup>H} NMR (150 MHz, DMSO-*d*<sub>6</sub>, 295 K, paramagnetic):  $\delta$  1010.8 (OAc), 963.3 (C3), 581.9 (C4), 576.1 (C6), 518.8 (C8), 471.2 (C12), 212.4 (C1), 208.2 (C2), 91.0 (C11), 66.6 (C9), 41.8 (C10), 15.1 (C7), -52.1 (C13), -217.7 (C5). HR-MS (FAB+) *m/z* (%): Calc. for C<sub>26</sub>H<sub>24</sub>CoN<sub>5</sub><sup>+</sup> ([M-OAc]<sup>+</sup>) 465.1364; Found 465.1376 (100).

**Computational details.** NMR shift calculations were performed using the spin unrestricted B3LYP density functional<sup>17</sup> as implemented in the Gaussian 09 program package.<sup>24</sup> Larger triple-zeta-valence plus polarisation<sup>18</sup> basis sets were used for the metal atoms and 6-311g(d,p)<sup>19</sup> basis sets for the non-metal atoms. The molecular systems studied were optimised starting from X-ray diffraction data without any symmetry restrictions. Stationary points on the potential energy surface

were characterised as minima by the absence of imaginary frequencies. During the calculations the spin contamination was controlled. Values of  $\langle S^2 \rangle$  only slightly deviated from the expected value.

### X-ray crystal structure determinations

Crystal data and details of the structure determinations are listed in Table 1. Intensity data were collected at low temperature (100 K) with a Bruker AXS Smart 1000 CCD diffractometer (Mo-K $\alpha$  radiation, graphite monochromator, *l* = 0.71073 Å). Data were corrected for air and detector absorption, Lorentz and polarisation effects;<sup>25</sup> absorption by the crystal was treated numerically or with a semiempirical multiscan method.<sup>26,27</sup>

The structures were solved by conventional direct methods (compound **1**)<sup>28,29</sup> or by the charge flip procedure (all others)<sup>30,31</sup> and refined by full-matrix least squares methods based on *F*<sup>2</sup> against all unique reflections.<sup>28,29</sup> All non-hydrogen atoms were given anisotropic displacement parameters. For the Fe and Co complexes hydrogen atoms were placed at calculated positions and refined with a riding model. For compounds **1** and **2** the positions of all hydrogen atoms were taken from difference Fourier syntheses and refined. Disorder of the methylene groups of the tetrahydroquinoline moieties was found in the complexes **3b** and **4**. The crystal solvent DMSO molecule in **3b-DMSO** and one of the acetate ligands in **4** were also disordered. All disorder was treated with split-atom models, applying geometry restraints when necessary.

CCDC 821499–821503 contains the supplementary crystallographic data for this paper.† These data can be obtained free of charge from The Cambridge Crystallographic Data Centre *via* www.ccdc.cam.ac.uk/data\_request/cif.

## Acknowledgements

We thank the Deutsche Forschungsgemeinschaft for funding and the Studienstiftung des Deutschen Volkes for a doctoral fellowship (to D. C. S.).

## References

- 1 See for example: (a) R. M. Bullock, *Angew. Chem., Int. Ed.*, 2007, **46**, 7360; (b) S. Enthaler, K. Junge and M. Beller, *Angew. Chem., Int. Ed.*, 2008, **47**, 3317; (c) C. Bolm, J. Legros, J. Le Pailh and L. Zani, *Chem. Rev.*, 2004, **104**, 6217; (d) M. Carril, A. Correa and C. Bolm, *Angew. Chem., Int. Ed.*, 2008, **47**, 4862; (e) S. C. Bart, E. Lobkovsky and P. J. Chirik, *J. Am. Chem. Soc.*, 2004, **126**, 13794; (f) A. M. Archer, M. W. Bouwkamp, M.-P. Cortez, E. Lobkovsky and P. J. Chirik, *Organometallics*, 2006, **25**, 4269; (g) R. J. Trovitch, E. Lobkovsky and P. J. Chirik, *Inorg. Chem.*, 2006, **45**, 7252; (h) S. C. Bart, E. J. Hawrelak, E. Lobkovsky and P. J. Chirik, *Organometallics*, 2005, **24**, 5518; (i) H. Egami and T. Katsuki, *J. Am. Chem. Soc.*, 2007, **129**, 8940; (j) K. P. Bryliakov and E. P. Talsi, *Angew. Chem.*, 2004, **116**, 5340; (k) M. Bullock, *Catalysis without precious metals*, Wiley-VCH Weinheim, 2010.
- 2 See for example: (a) P. Di Bernardo, A. Melchior, R. Portanova, M. Tolazzi and P. L. Zanonato, *Coord. Chem. Rev.*, 2008, **252**, 1270; (b) C. A. Caputo and N. D. Jones, *Dalton Trans.*, 2007, 4627; (c) T. P. Yoon and E. N. Jacobsen, *Science*, 2003, **299**, 1691; G. Desimoni, G. Faita and P. Quadrelli, *Chem. Rev.*, 2003, **103**, 3119; (d) M. Gómez, G. Muller and M. Rocamora, *Coord. Chem. Rev.*, 1999, **193–195**, 769; (e) N. C. Fletcher, *J. Chem. Soc., Perkin Trans. 1*, 2002, 1831; (f) S. D. Ittel, L. K. Johnson and M. Brookhart, *Chem. Rev.*, 2000, **100**, 1169; (g) L. M. Rendina and R. J. Puddephatt, *Chem. Rev.*, 1997, **97**, 1735; (h) T. Katsuki, *Coord. Chem. Rev.*, 1995, **140**, 189.
- 3 Reviews covering “pincer” complex chemistry: (a) M. Albrecht and G. van Koten, *Angew. Chem., Int. Ed.*, 2001, **40**, 3750; (b) M. von der Boom and D. Milstein, *Chem. Rev.*, 2003, **103**, 1759; (c) H. Nishiyama, *Chem. Soc. Rev.*, 2007, **36**, 1133.
- 4 (a) J. A. Elvidge and R. P. Linstead, *J. Chem. Soc.*, 1952, 5000; (b) J. A. Elvidge and R. P. Linstead, *J. Chem. Soc.*, 1952, 5008; (c) P. F. Clark, J. A. Elvidge and R. P. Linstead, *J. Chem. Soc.*, 1953, 3593.
- 5 (a) R. R. Gagné, W. A. Marritt, D. N. Marks and W. O. Siegl, *Inorg. Chem.*, 1981, **20**, 3260; W. O. Siegl, *Inorg. Chim. Acta*, 1977, **25**, L65; (b) R. R. Gagné, R. S. Gall, G. S. Lisensky, R. E. Marsh and L. M. Speltz, *Inorg. Chem.*, 1979, **18**, 771; (c) D. N. Marks, W. O. Siegl and R. R. Gagné, *Inorg. Chem.*, 1982, **21**, 3140; (d) M. B. Meder, C. H. Galka and L. H. Gade, *Monatsh. Chem.*, 2005, **136**, 1693; (e) M. Bröring, C. Kleeberg and S. Köhler, *Inorg. Chem.*, 2008, **47**, 6404; (f) B. K. Langlotz, J. Lloret Fillol, J. H. Gross, H. Wadepohl and L. H. Gade, *Chem.–Eur. J.*, 2008, **14**, 10267.
- 6 (a) W. O. Siegl, *Inorg. Nucl. Chem. Lett.*, 1974, **10**, 825; (b) W. O. Siegl, *J. Organomet. Chem.*, 1976, **107**, C27; (c) W. O. Siegl, *J. Org. Chem.*, 1977, **42**, 1872; (d) L. Saussine, E. Brazi, A. Robine, H. Mimoun, J. Fischer and R. Weiss, *J. Am. Chem. Soc.*, 1985, **107**, 3534; (e) C. A. Tolman, J. D. Druliner, P. J. Krusic, M. J. Nappa, W. C. Seidel, I. D. Williams and S. D. Ittel, *J. Mol. Catal.*, 1988, **48**, 129.
- 7 (a) B. Siggelkow, M. B. Meder, C. H. Galka and L. H. Gade, *Eur. J. Inorg. Chem.*, 2004, 3424; (b) B. A. Siggelkow and L. H. Gade, *Z. Anorg. Allg. Chem.*, 2005, **631**, 2575.
- 8 J. A. Camerano, C. Sämman, H. Wadepohl and L. H. Gade, *Organometallics*, 2011, **30**, 379.
- 9 B. K. Langlotz, H. Wadepohl and L. H. Gade, *Angew. Chem., Int. Ed.*, 2008, **47**, 4670.
- 10 In contrast, most of the “homoleptic”  $[M(\text{bpi})_2]$  complexes are well-known, including their structural features. These systems are usually substitutionally inert and therefore unsuitable as catalysts: (a) M. A. Robinson, S. I. Trotz and T. H. Hurley, *Inorg. Chem.*, 1967, **6**, 392; (b) P. J. Domaille, R. L. Harlow, S. D. Ittel and W. G. William, *Inorg. Chem.*, 1983, **22**, 3944; (c) M. B. Meder, B. A. Siggelkow and L. H. Gade, *Z. Anorg. Allg. Chem.*, 2004, **630**, 1962; (d) É. Balogh-Hergovich, G. Speier, M. Réglér, M. Giorgi, E. Kuzmann and A. Vértes, *Inorg. Chem. Commun.*, 2005, **8**, 457; (e) M. Wicholas, A. D. Garrett, M. Gleaves, A. M. Morris, M. Rehm, O. P. Anders and A. la Cour, *Inorg. Chem.*, 2006, **45**, 5804; (f) J. Kaizer, G. Baráth, R. Csonka, G. Speier, L. Korecz, F. Rockenbauer and L. Párkányi, *J. Inorg. Biochem.*, 2008, **102**, 773; (g) P. T. Solvi, H. Stoeckli-Evans and M. Palaniandavar, *J. Inorg. Biochem.*, 2005, **99**, 2110.
- 11 M. B. Meder and L. H. Gade, *Eur. J. Inorg. Chem.*, 2004, 2716.
- 12 A. R. Rossi and R. Hoffmann, *Inorg. Chem.*, 1975, **14**, 365.
- 13 (a) G. N. La Mar, W. DeW. Horrocks Jr., R. H. Holm, (ed.); *NMR of Paramagnetic Molecules*, Academic Press, New York, 1973; (b) I. Bertini and C. Luchinat, *Coord. Chem. Rev.*, 1996, **150**, 1; (c) F. H. Köhler, *Magnetism: Molecules to Materials*, ed. J. S. Miller, M. Drillon, Wiley-VCH, Weinheim, 2001, p. 379–430; (d) I. Bertini, C. Luchinat and G. Parigi, *Prog. Nucl. Magn. Reson. Spectrosc.*, 2002, **40**, 249; (e) I. Bertini, C. Luchinat, G. Parigi and R. Pierattelli, *ChemBioChem*, 2005, **6**, 1536; (f) F. Rastrelli and A. Bagno, *Chem.–Eur. J.*, 2009, **15**, 7990; (g) M. Kaupp and F. H. Köhler, *Coord. Chem. Rev.*, 2009, **253**, 2376.
- 14 (a) T. O. Pennanen and J. Vaara, *Phys. Rev. Lett.*, 2008, **100**, 133002; (b) H. Liimatainen, T. O. Pennanen and J. Vaara, *Can. J. Chem.*, 2009, **87**, 954.
- 15 (a) J. Mao, Y. Zhang and E. Oldfield, *J. Am. Chem. Soc.*, 2002, **124**, 13911; (b) R. Knorr, H. Hauer, A. Weiss, H. Polzer, F. Ruf, P. Löw, P. Dvortsák and P. Böhrer, *Inorg. Chem.*, 2007, **46**, 8379.
- 16 (a) P. Fernández, H. Pritzkow, J. Carbó, P. Hofmann and M. Enders, *Organometallics*, 2007, **26**, 4402; (b) P. Roquette, A. Maronna, M. Reinmuth, E. Kaifer, M. Enders and H.-J. Himmel, *Inorg. Chem.*, 2011, **50**, 1942.
- 17 (a) A. D. Becke, *J. Chem. Phys.*, 1993, **98**, 5648; (b) C. Lee, W. Yang and R. G. Parr, *Phys. Rev. B*, 1988, **37**, 785.
- 18 (a) A. Schäfer, C. Huber and R. Ahlrichs, *J. Chem. Phys.*, 1994, **100**, 5829; (b) F. Weigend and R. Ahlrichs, *Phys. Chem. Chem. Phys.*, 2005, **7**, 3297.
- 19 (a) M. M. Francl, W. J. Pietro, W. J. Hehre, J. S. Binkley, M. S. Gordon, D. J. Defrees and J. A. Pople, *J. Chem. Phys.*, 1982, **77**, 3654; (b) W. J. Hehre, R. Ditchfield and J. A. Pople, *J. Chem. Phys.*, 1972, **56**, 2257; (c) P. C. Hariharan and J. A. Pople, *Theor. Chim. Acta*, 1973, **28**, 213.
- 20 The calculated Mulliken spin densities reflect the total spin density within the space around the corresponding atom, whereas the Fermi-contact shift is a consequence of the spin density at the atom nucleus only (i.e. MO's with s-atomic orbital contribution). Due to the different pathways of spin delocalisation the Mulliken spin densities and the Fermi-contact shifts are not correlated in a linear manner and may even show opposite signs.
- 21 D. F. Evans, *J. Chem. Soc.*, 1959, 2003.
- 22 (a) T. J. J. Sciarone, A. Meetsma and B. Hessen, *Inorg. Chim. Acta*, 2006, **359**, 1815; (b) J. Scott, S. Gambrotta, I. Korobkov and P. H. M. Budzelaar, *J. Am. Chem. Soc.*, 2005, **127**, 13019; (c) A. M. Archer, M. W. Bouwkamp, M.-P. Cortez, E. Lobkovsky and P. J. Chirik, *Organometallics*, 2006, **25**, 4269.
- 23 R. J. Vijn, H. J. Arts, P. J. Maas and A. M. Castelijns, *J. Org. Chem.*, 1993, **58**, 887.
- 24 *Gaussian 09*, Revision A.02, M. J. Frisch, G. W. Trucks, H. B. Schlegel, G. E. Scuseria, M. A. Robb, J. R. Cheeseman, G. Scalmani, V. Barone, B. Mennucci, G. A. Petersson, H. Nakatsuji, M. Caricato, X. Li, H. P. Hratchian, A. F. Izmaylov, J. Bloino, G. Zheng, J. L. Sonnenberg, M. Hada, M. Ehara, K. Toyota, R. Fukuda, J. Hasegawa, M. Ishida, T. Nakajima, Y. Honda, O. Kitao, H. Nakai, T. Vreven, J. A. Montgomery, Jr., J. E. Peralta, F. Ogliaro, M. Bearpark, J. J. Heyd, E. Brothers, K. N. Kudin, V. N. Staroverov, R. Kobayashi, J. Normand, K. Raghavachari, A. Rendell, J. C. Burant, S. S. Iyengar, J. Tomasi, M. Cossi, N. Rega, J. M. Millam, M. Klene, J. E. Knox, J. B. Cross, V. Bakken, C. Adamo, J. Jaramillo, R. Gomperts, R. E. Stratmann, O. Yazyev, A. J. Austin, R. Cammi, C. Pomelli, J. W. Ochterski, R. L. Martin, K. Morokuma, V. G. Zakrzewski, G. A. Voth, P. Salvador, J. J. Dannenberg, S. Dapprich, A. D. Daniels, O. Farkas, J. B. Foresman, J. V. Ortiz, J. Cioslowski and D. J. Fox, Gaussian Inc., Wallingford CT, 2009.
- 25 *SAINT*, Bruker AXS, 1997–2008.
- 26 R. H. Blessing, *Acta Crystallogr., Sect. A: Found. Crystallogr.*, 1995, **51**, 33.
- 27 G. M. Sheldrick, *SADABS*, Bruker AXS, 2004–2008.
- 28 G. M. Sheldrick, *Acta Crystallogr., Sect. A: Found. Crystallogr.*, 2007, **64**, 112.
- 29 G. M. Sheldrick, *Acta Crystallogr., Sect. A: Found. Crystallogr.*, 1990, **46**, 467.
- 30 (a) G. Oszlányi and A. Sütö, *Acta Cryst.*, 2004, **A60**, 134; (b) G. Oszlányi and A. Sütö, *Acta Crystallogr., Sect. A: Found. Crystallogr.*, 2004, **61**, 147.
- 31 L. Palatinus, *SUPERFLIP*, EPF Lausanne, Switzerland, 2007; L. Palatinus and G. Chapuis, *J. Appl. Crystallogr.*, 2007, **40**, 786.